

High-pressure and high-temperature equation of state and phase diagram of solid benzene

Lucia Ciabini,^{1,2} Federico A. Gorelli,^{1,3,*} Mario Santoro,^{1,†} Roberto Bini,^{1,2,‡} Vincenzo Schettino,^{1,2} and Mohamed Mezouar⁴

¹LENS, European Laboratory for Non-linear Spectroscopy and INFN, Via Carrara 1, I-50019 Sesto Fiorentino, Firenze, Italy

²Dipartimento di Chimica dell'Università di Firenze, Via della Lastruccia 3, I-50019 Sesto Fiorentino, Firenze, Italy

³INFN-CRS SOFT, Università di Roma La Sapienza, Piazza A. Moro 2, I-00185, Roma, Italy

⁴European Synchrotron Research Facility, Boîte Postale 220, F38043 Grenoble, France

(Received 31 January 2005; published 13 September 2005)

The high-pressure structural properties of benzene have been investigated up to the occurrence of the chemical reaction by means of x-ray diffraction and infrared absorption techniques. The infrared spectra show that sample annealing above 500 K produces pure phase-II crystals. X-ray diffraction patterns collected at 540 K on these crystals allowed the equation of state of benzene to be obtained. These results indicate the stability of phase II up to the pressure where benzene reacts and no evidence of the III and III' crystal structures is gained. On these bases the existing phase diagram of benzene is discussed and a simplified one is proposed.

DOI: [10.1103/PhysRevB.72.094108](https://doi.org/10.1103/PhysRevB.72.094108)

PACS number(s): 61.50.Ks, 78.30.-j

I. INTRODUCTION

Since a few decades high-pressure physics and chemistry are appealing fields to set innovative strategies to synthesize new materials of technological interest. Historically, the search for new superhard materials, such as synthetic diamonds or cubic boron nitride (*c*-BN), has represented the driving area in the field, but promising results have been obtained also in the synthesis of optical and optoelectronic materials, polymers, and amorphous compounds.¹⁻³ While the interest for polymers is essentially bound to the innovative preparation method based on the photoactivation of a high-pressure reaction in the pure monomer,^{4,5} the preparation of entirely new high-density amorphous materials, made of carbon or other light atoms, attracts considerable interest for their great technological potential. In this framework, the formation of amorphous hydrogenated carbons (*a*-C:H) by compressing simple unsaturated (CH)_{*n*} hydrocarbons such as acetylene^{6,7} and benzene is particularly relevant. For these systems the steep increase in the intermolecular interactions, determined by the application of a suitable external pressure, is joined to the high reactivity of the π bonds: the opening of double and triple bonds originates radical species that trigger chain reactions. In benzene, the prototype of the aromatic compounds, the stability of the aromatic ring requires pressures of some tenths of gigapascals and/or temperatures as high as hundreds of degrees Celsius for the reaction to occur. Nevertheless, the transformation of benzene under pressure is one of the most extensively studied examples of pressure-induced reactivity in hydrocarbons.⁸⁻¹⁸

In order to understand the mechanism driving a solid state reaction knowledge of the crystal structure and of the relative orientations and distances among the molecules is mandatory. Although benzene represents the prototype of aromatic compounds, its structural characterization at high pressure is far from being complete. In the most recent phase diagram the boundaries between the different crystal phases have been drawn by using Raman spectroscopy, and specifically the linewidth evolution of the breathing mode as a function of pressure at different temperatures.¹⁵ Among the five crys-

tal phases proposed for solid benzene only the structure of phase I, which is obtained by freezing the liquid at room pressure or compressing it above 700 bar at room temperature, is univocally accepted: orthorhombic *Pbca* (D_{2h}^{15}).^{19,20} At room temperature and 1.4 GPa the transition to phase II occurs. The structure of this phase, indicated to be stable up to 4 GPa, was determined by single-crystal x-ray diffraction experiments as monoclinic $P2_1/c(C_{2h}^5)$ with two molecules per unit cell.²¹ The existence of another high-pressure crystal phase was suggested on the basis of visual observation⁹ and differential thermal analysis.²² The existence of this phase (III) at room temperature was later confirmed, on the basis of Raman and x-ray diffraction data, between 4 and 11 GPa.¹¹ The room-temperature diffraction pattern observed in this study consisted of only eight poorly resolved lines that could not be assigned, between 1.4 and 4 GPa, by using the $P2_1/c$ structure proposed by Piermarini *et al.* for phase II.²¹ On the other hand, the $P2_1/c$ structure was found to fit nicely the measured pattern above 4 GPa in the presumed new phase III. Therefore, Thiéry and Legér¹¹ concluded that an inaccurate pressure determination led Piermarini *et al.* to assign to phase II the structure of phase III. Both I-II and II-III phase transitions were found to be extremely sluggish, while they were speeded up by heating the sample.¹¹ Raman^{11,23-25} and ir experiments^{24,26,27} provided some indications of the I-II phase transition, consisting of spectral changes and discontinuities in the pressure evolution of the phonon frequencies. On the contrary, the II-III phase transition, apart from the already mentioned anomalous behavior with pressure of the linewidth of the breathing mode,¹⁵ is inferred only from small slope changes in the pressure shift of the lattice and some internal vibrational modes.^{11,25,27} Around 11 GPa Thiéry *et al.*¹¹ report a change in the pressure dependence of the lattice parameters which is attributed to a second-order transition to a new phase (III'), having probably the same monoclinic structure as phase III. Also in this case very small slope changes in the frequency^{11,27} and linewidth¹⁵ evolution with pressure have been reported. Finally, above 20 GPa both the x-ray diffraction pattern and the vibrational spectrum change as a consequence of the chemical transforma-

tion of benzene.^{8,11,15} This reaction, studied both at high^{9,15} and room^{8,16} temperature, consists of the opening of the aromatic ring which leads to the formation of an amorphous hydrogenated carbon with peculiar characteristics, such as a high optical gap and the absence of graphitic regions, in comparison to that obtained by other common preparation techniques such as chemical vapor deposition.^{16,18} The same reaction was later successfully induced at room temperature, but at lower (15 GPa) pressure, by optical excitation of the S_1 state,¹⁷ thus suggesting an active role of the excited electronic states in the reaction mechanism.

In the attempt to investigate the high-pressure phase diagram of benzene we performed a high-temperature x-ray diffraction and ir absorption study up to 540 K and 26 GPa. The high-temperature equation of state (EOS) and the pressure dependence of the cell parameters were determined, allowing a more precise characterization of the phase diagram which greatly simplifies the existing one.¹⁵

II. EXPERIMENTAL SETUP

High-pressure x-ray diffraction patterns and infrared absorption spectra of solid benzene were measured using a membrane diamond anvil cell equipped with IIa diamonds. The cell was loaded by filling the gasket hole with a drop of liquid benzene from Merck (purity $\geq 99.9\%$). The initial sample dimensions were typically 40–50 μm thick and 150 μm in diameter and either a rhenium or stainless steel gasket was employed to retain the sample. In high-temperature experiments the formation of large high-quality crystals is generally observed and a good quality of the ir spectrum achieved. On the other hand, a reliable analysis of the x-ray diffraction pattern is prevented by large crystalline domains having preferred orientations. In the present study, we succeeded in producing a fine powder by rapidly compressing the sample several times through the I-II phase transition. A considerable reduction of the texture was not possible when phase II was produced at high temperature directly from the liquid ($T > 480$ K). A ruby chip was inserted in the sample to measure the local sample pressure by the R_1 ruby fluorescence band shift according to the equation P (GPa) = $248.4[(\Delta\lambda/\lambda_0 + 1)^{7.665} - 1]$.²⁸ The term $\Delta\lambda$ accounts for the ruby luminescence shift with respect to ambient pressure and temperature conditions according to the relation $\Delta\lambda = (\lambda - \lambda_0) - \Delta\lambda_T$, where $\Delta\lambda_T$ is a third-order polynomial with coefficients $c_1 = 0.0739 \text{ \AA K}^{-1}$, $c_2 = -2.6 \times 10^{-5} \text{ \AA K}^{-2}$, $c_3 = 8.3 \times 10^{-8} \text{ \AA K}^{-3}$. Temperatures up to 540 K were obtained by a resistive heating of the cell. The temperature was measured by a J-type thermocouple placed close to the copper ring that clamps the diamond anvil. The uncertainty on the temperature measurements is estimated to be 3 K. The apparatus to perform infrared experiments under pressure, including the optical beam condenser, has been described elsewhere.^{29,30} A Fourier transform infrared spectrometer (Bruker IFS-120 HR) was used to measure the infrared absorption spectra. The instrument was equipped with different beam splitters and detectors to cover the frequency region from 50 to 4000 cm^{-1} . The instrumental resolution was better than 1 cm^{-1} . Angle-dispersive x-ray diffraction

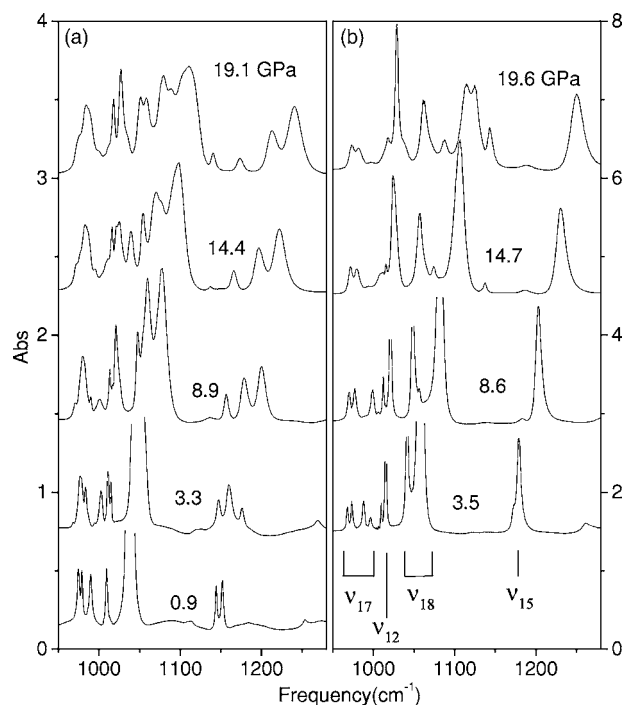


FIG. 1. Comparison of the ir spectra in the region of the ν_{17} , ν_{12} , ν_{18} , and ν_{15} internal modes measured at room temperature along compression experiments: (a) in a not-annealed sample; (b) after annealing at 2 GPa up to 500 K. The spectrum reported in the (a) panel at 0.9 GPa is measured in the orthorhombic phase I.

(ADXRD) patterns have been measured at the ID30 beamline of the European Synchrotron Radiation Facility (ESRF, Grenoble), with monochromatic beam ($\lambda = 0.3738 \text{ \AA}$), and image plate detection. The nominal size of the focal spot was equal to $10 \times 10 \mu\text{m}^2$. The diffraction patterns were integrated and analyzed by means of the FIT2D computer code,³¹ to obtain the one-dimensional intensity distribution as a function of the 2θ scattering angle.

III. INFRARED ANALYSIS

One of the more relevant limitations in the study of the phase diagram of benzene is the strong metastability of the orthorhombic phase I within the P - T domain of the higher-pressure phase. The complete removal of phase I is claimed to be obtained when the sample is annealed above 373 K.¹¹ In Fig. 1 we compare a portion of the ir spectra of samples compressed at room temperature (a) without annealing procedure and (b) after annealing at 500 K and 2 GPa beyond the I-II phase boundary. In Fig. 1(a) a spectrum measured at 0.9 GPa in the orthorhombic $Pbca$ phase I is also reported. By comparing the spectra recorded in the two different samples at nearly equal pressures, it can be seen that all the modes show, in the annealed sample, a decreased number of sharper components. This is particularly evident for the isolated ν_{15} C-H bending mode at $\sim 1180 \text{ cm}^{-1}$. In the annealed sample only the two expected crystal components for a monoclinic cell with two molecules in the unit cell are observed, even though partly overlapped. On the contrary, a

triplet is observed in the not-annealed sample indicating the coexistence of the orthorhombic (to which the two low-frequency bands belong) and monoclinic phases (revealed by the higher-frequency band). It is remarkable that the coexistence is not removed at higher pressure and persists up to the threshold of the chemical transformation of benzene. The relative intensities of these bands change during the sample compression indicating a sluggish conversion to the monoclinic phase, which is the stable form at high pressure. The same behavior is also shown by all the other internal modes where the intensity gain of the monoclinic bands is only observed well above the I-II transition pressure (1.4 GPa).

The appearance of the absorption pattern due to C-H stretching modes of saturated carbon atoms, which is the signature of the chemical reaction, is observed at 21–22 GPa when the sample is compressed at 540 K. This pressure value is in fair agreement with that reported by Cansell *et al.* and determined by the Raman spectra of the ν_1 breathing mode.¹⁵

The lattice phonon spectrum was also measured during a compression run at 450 K. Three translational modes are expected in the ir spectrum of the monoclinic phase, but only one peak is observed at this temperature corresponding to the high-frequency band measured in a previous room-temperature experiment.²⁷ This sample was decompressed at room temperature after that the maximum pressure of 15.2 GPa, lower than the reaction threshold pressure, was reached. At 300 K a second weak peak is observed at lower frequency. The spectra and the pressure shift of the lattice phonons are compared to that measured in a room-temperature pressurization where the sample was not thermally annealed²⁷ in Figs. 2 and 3, respectively. A fair agreement is found in the pressure range of interest; the main differences are related to the missed observation of the central band reported in the not-annealed sample, and to the stronger pressure dependence of the low-frequency peak. The central band, not observed in all the experiments performed at room temperature, was correlated to a higher crystal quality.²⁷ On the contrary, the present results, which indeed are obtained on high-quality crystals, since the pressurization is performed at high temperature, indicate that this band should be rather related to the presence of the metastable phase I. This conclusion is supported by the following points. This band corresponds to the strongest peak of phase I, and it weakens on increasing pressure as opposite to the intensification of the other two bands.²⁷ Also the slight slope change²⁷ identified for the low-frequency mode at about 11–12 GPa is not confirmed by the present study thus casting a shadow on the presence of the II-III and III-III' phase transitions.

IV. X-RAY DIFFRACTION ANALYSIS

The coexistence between phase I and the higher-pressure phases can prevent a reliable interpretation of the x-ray diffraction data. This could be the reason for the missed confirmation of the structure proposed by Piermarini *et al.*²¹ for phase II in the later work by Thiéry *et al.*¹¹ Also our ir results show that annealing cycles and high-temperature studies are

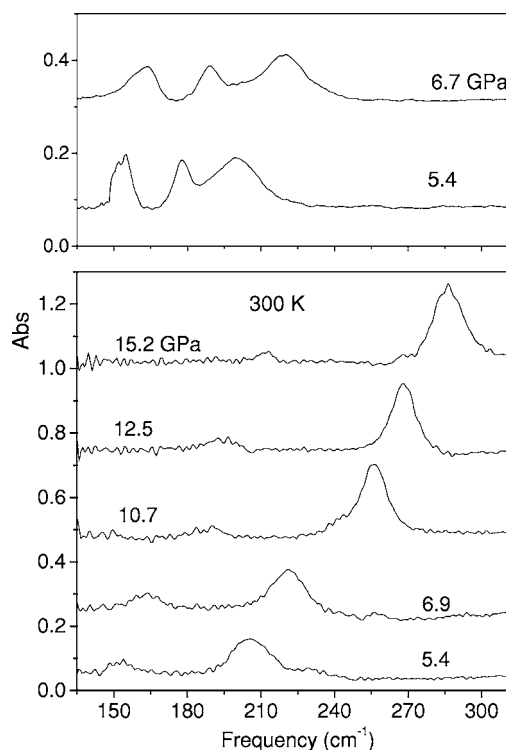


FIG. 2. Room-temperature far-infrared spectra of solid benzene measured during decompression in a not-annealed sample (upper panel) and in an annealed sample (lower panel).

mandatory to gain precise structural information. After preparing powdered samples according to the procedure described in the experimental section, we collected the diffraction pattern at 540 K both during compression experiments, where the sample was allowed to react, and in compression-decompression cycles, below the reaction pressure threshold. In Fig. 4 we report two ADXD patterns measured at 3.0 and 20.7 GPa. The nearly homogeneous diffraction rings show

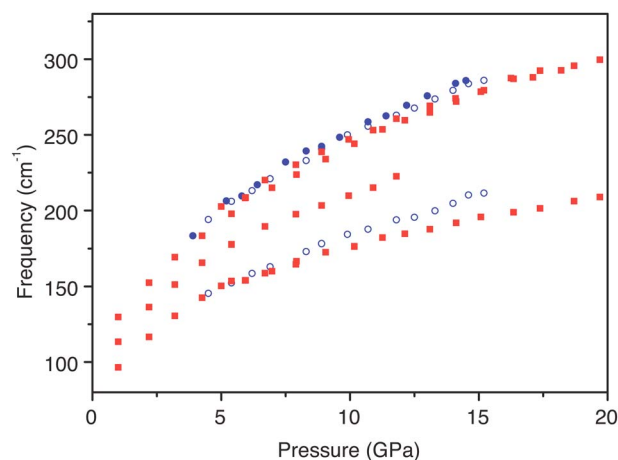


FIG. 3. (Color online) Comparison of the room-temperature pressure shift of the phonon bands measured in the annealed sample (empty dots, decompression at 300 K; full dots, compression at 450 K) and in the room-temperature experiment on a not-annealed sample reported in Ref. 27 (full squares).

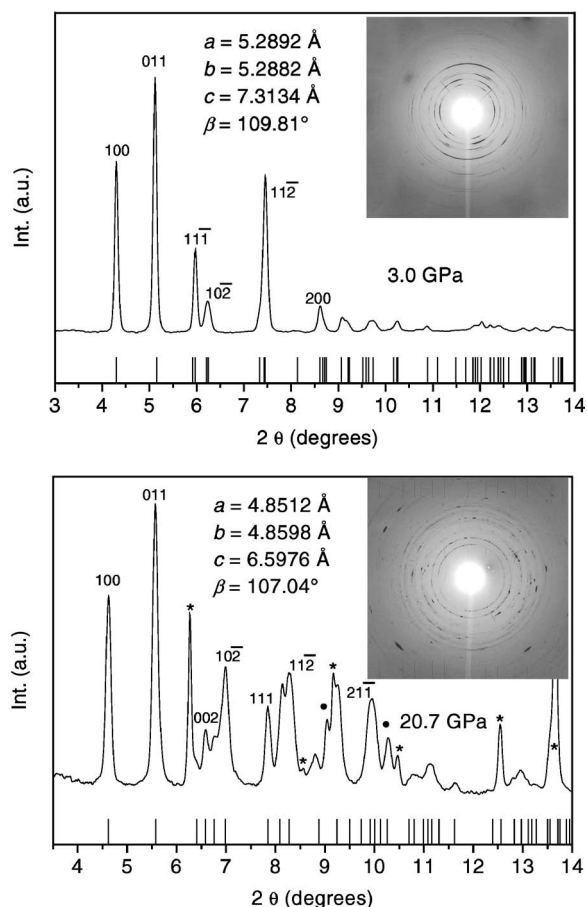


FIG. 4. Two-dimensional x-ray diffraction patterns (inset), and intensity distribution as a function of the 2θ scattering angle, measured at 540 K on different samples at 3.0 and 20.7 GPa, respectively. The calculated peak positions according to the $P2_1/c$ monoclinic structure, drawn as vertical bars and the assignment of the most intense diffraction lines are also reported. Lines due to ruby and rhenium are indicated by stars and circles, respectively.

that a randomly oriented powdered sample has been obtained. Nevertheless, a slight residual texture does not allow data refinement for determining the atomic positions. The diffraction patterns have been acquired by scanning and averaging the signals from different sections of the sample. This procedure caused, in some experiments and especially at high pressure, the presence in our patterns of the ruby and rhenium (from the gasket) diffraction lines. These peaks are easily identified and discarded for the structure analysis. Possible structures were searched using a minimum of 18 and a maximum of 25 reflections, depending on pressure, assigned to crystalline benzene. A good agreement between the measured diffraction peaks and the expected reflection positions is found, in the investigated pressure range (1–26 GPa), only by indexing the diffraction pattern with the monoclinic $P2_1/c$ unit cell. The calculated diffraction lines for this crystal structure are also shown in Fig. 4 together with the assignment of the most intense lines. The experimental and calculated d spacings are reported at two pressures in Table I. In Fig. 5 we have reported the pressure evolution of the diffraction pattern measured from 1.7 GPa, close to the melt-

TABLE I. Assignment according to the $P2_1/c$ crystal structure of the observed diffraction lines at two different pressures. The calculated and experimental d spacings are reported and compared.

Reflection hkl	d_{hkl} Å (1.75 GPa)			d_{hkl} Å (10.8 GPa)		
	Calc.	Expt.	Δ	Calc.	Expt.	Δ
100	5.1335	5.1326	0.0009	4.7882	4.7986	-0.0104
011	4.3193	4.3180	0.0013	3.9942	3.9802	0.0140
110	3.7263	3.7330	-0.0067	3.4561	3.4660	-0.0099
$11\bar{1}$	3.7166	3.7179	-0.0013	3.3921	3.3953	-0.0032
$10\bar{2}$	3.5640	3.5623	0.0017	3.2041	3.2101	-0.0060
002	3.5528	3.5502	0.0026	3.2806	3.2750	0.0056
111	3.0045	3.0036	0.0009	2.8138	2.8132	0.0006
$11\bar{2}$	2.9815	2.9801	0.0014	2.6928	2.7031	-0.0103
012	2.9745	2.9730	0.0015	2.7325	2.7415	-0.0090
020	2.7201	2.7197	0.0004	2.4936	2.5058	-0.0122
200	2.5706	2.5663	0.0043	2.3954	2.3993	-0.0039
$20\bar{2}$		2.5465		2.3082		
021	2.5414	2.5397	0.0017	2.3355	2.3404	-0.0049
102	2.5309	2.5335	-0.0026	2.3848	2.3818	0.0030
$21\bar{1}$	2.4475	2.4472	0.0003	2.2523	2.2518	0.0005
120	2.4035	2.4031	0.0004	2.2229	2.2212	0.0017
$12\bar{1}$	2.3981	2.3991	-0.0010	2.2083	2.2023	0.0060
210	2.3179	2.3209	-0.0030	2.1639	2.1641	-0.0002
$21\bar{2}$	2.3067	2.3064	0.0003	2.1000	2.0965	0.0035
112	2.2978	2.2966	0.0012	2.1509	2.1512	-0.0003
$11\bar{3}$	2.2771	2.2791	-0.0020	2.0723	2.0690	0.0033
cell parameters (1.75 GPa)		cell parameters (10.8 GPa)				
a	5.4808 Å			5.0495 Å		
b	5.4393 Å			5.0116 Å		
c	7.5822 Å			6.8925 Å		
β	110.53			108.14		

ing point, up to 23.5 GPa before the occurrence of the chemical reaction. From the figure it is evident that two groups of lines (6° and 7.2°) are difficult to resolve at low pressure but progressively separate during the compression, thus favoring their assignment. As a whole, our results, which are based on a much larger number of observed and assigned reflections with respect to previous studies,¹¹ indicate the persistence of the same crystal structure up to the occurrence of the chemical reaction. This structure was originally proposed for phase II by Piermarini *et al.*²¹ and later ruled out by Thiéry *et al.*,¹¹ who in turn assigned it to phase III. The discrepancy can be possibly due to an ineffective annealing, performed at only 373 K in Ref. 11, so that phase I was not completely removed, preventing a reliable interpretation of the x-ray diffraction data. On the other hand, phase II was prepared by Piermarini *et al.*²¹ above 550 K, as we did in our procedure. More recently, classical molecular dynamics calculations simulating the packing in the high-pressure crystal phases of benzene found the $P2_1/c$ structure to be the stablest one also in the P - T region corresponding to phase II.³²

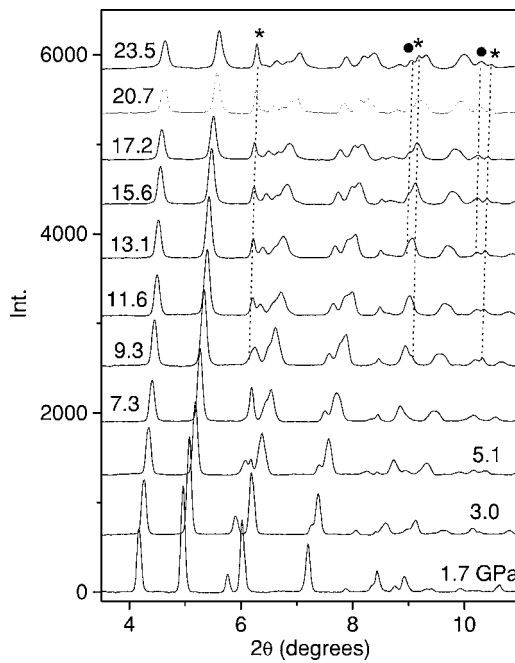


FIG. 5. Evolution with pressure of the x-ray diffraction patterns measured in a compression experiment at 540 K. Lines due to ruby and rhenium are indicated by stars and circles, respectively, while the dotted lines are just guides for the eye to follow their evolution.

The evolution with pressure of the cell parameters a, b, c and the monoclinic angle β is reported in Fig. 6. The data are relative to two different experiments: in one case the sample has been decompressed below the threshold pressure of the chemical reaction, while in the other case we let the reaction take place. In the latter case the general observation of a good diffraction pattern at pressures above the reaction threshold pressure (21–22 GPa at 540 K), estimated by the observation of the stretching modes involving saturated C atoms, should be remarked. As a matter of fact, only above 26 GPa do most of the diffraction lines disappear while the remaining peaks become very broad. A nice agreement is found in the two experiments concerning the values of the c and β parameters, while a difference, that increases on rising pressure, results for a and b . This produces a different pressure evolution of the volume (see Fig. 7). These two sets of data have been fitted by a Vinet equation of state:³³

$$P = 3B_0 \frac{(1-f_\nu)}{f_\nu^2} \exp \left[\frac{3}{2} (C_0 - 1)(1-f_\nu) \right] \quad (1)$$

where $f_\nu = (V/V_0)^{1/3}$, V_0 being the cell volume at ambient pressure, and B_0 and C_0 the isothermal bulk modulus and its derivative against pressure at $P=0$, respectively. We could fit the pressure evolution of the volume by using the same V_0 and B_0 , while slightly different C_0 were employed in the two cases. This can be explained in terms of nonhydrostatic pressure and preferred orientation of the crystallites. The volume and lattice parameters values agree with those reported by Piermarini *et al.* at 2.5 GPa;²¹ on the contrary, their pressure evolution is markedly different from that reported in Ref. 11 especially as far as the β and c parameters are concerned. In

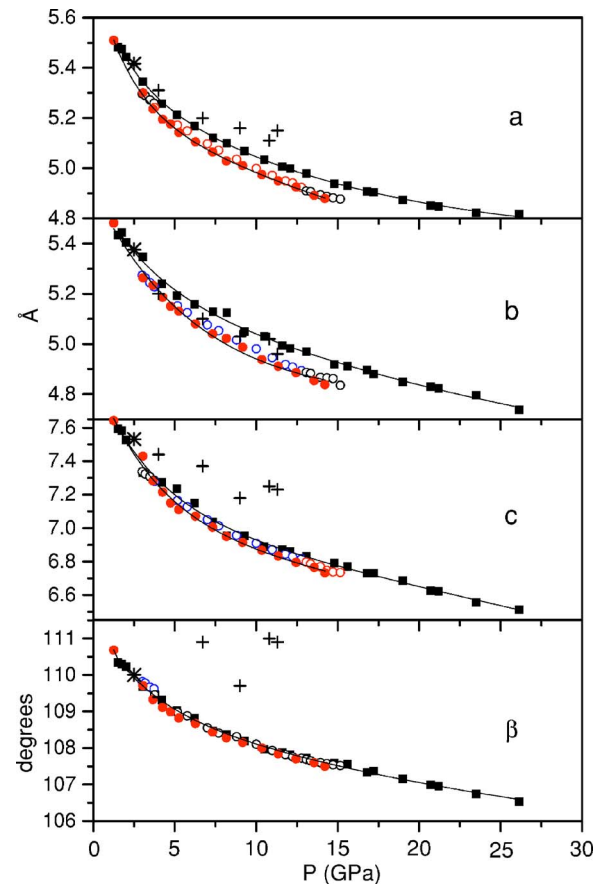


FIG. 6. (Color online) Pressure evolution measured at 540 K of the a, b, c lattice parameters and of the monoclinic angle β for a $P2_1/c$ unit cell. The two sets of data measured in the present work refer to the compression of the sample above the reaction threshold (full squares), and to compression (empty dots) and decompression (full dots) of the sample below the reaction threshold. Full lines are drawn to help the identification of the evolution of the different data sets. For comparison the room-temperature data from Refs. 21 (asterisk) and 11 (crosses) are also reported.

general, the pressure evolution of the lattice parameters and of the cell volume values measured in the present report is very regular, i.e., no discontinuities or slope change are noticed, and a nice agreement is found between the compression and decompression data. Therefore, no indications of the II-III and III-III' phase transitions are found in these experiments as also suggested by the ir measurements performed on annealed samples.

V. THE PHASE DIAGRAM

Our ir and x-ray diffraction experiments indicate that phase II is stable up to the chemical reaction while no indications of the existence of the phases III and III' have been found up to 540 K. Therefore, it appears mandatory to reconsider how the II-III and III-III' phase boundaries have been drawn. The II-III and III-III' phase transitions were detected, at 376 and 633 K, by a cusp minimum and a slope change, respectively, in the evolution of the linewidth (Γ) of the breathing mode (ν_1) with pressure.¹⁵ No other effects were

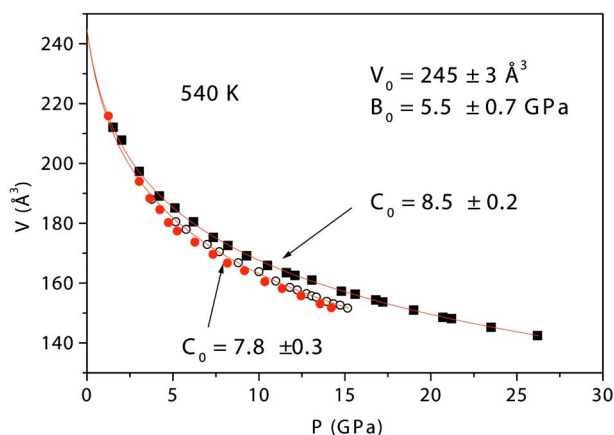


FIG. 7. (Color online) EOS of crystalline benzene at 540 K. The two sets of data (dots and squares) are relative to different samples. The data acquired during compression (empty dots) and decompression (full dots) are reported for the experiment where the onset of the chemical reaction was not reached. The evolution with pressure of the volume has been fitted by a Vinet equation [Eq. (1)] and the same values of V_0 and B_0 have been found for the two curves while C_0 differs in the two cases of about 10%.

detected in the pressure shift of this or other modes. The authors also stated that due to thermal oscillations during the long Raman spectra acquisitions and to the unresolved ν_1 doublet the measured linewidth values were likely strongly affected. Furthermore, the line narrowing of the ν_1 mode observed during the compression of the sample in phase II (Ref. 15) does not agree with the broadening measured by time-resolved stimulated Raman scattering in the same pressure range.³⁴

The employment of the linewidth pressure shift for identifying phase transitions is questionable since this parameter, or equivalently the lifetime of the mode under examination, reflects the entire crystal dynamics.³⁵ This means that beside phase transitions also changes of the mechanisms regulating the coupling with the other crystal phonons can give rise to an anomalous behavior of the evolution of the Γ values with pressure. A precise knowledge of the phonon density of states (DOS) and how it is modified by pressure, and of the active relaxation channels, inferred by studies of Γ vs T , is mandatory for a reliable discussion. A minimum in the linewidth evolution with pressure has been reported for the symmetric stretching mode (ν_1) of the NO_3^- ion in NaNO_3 and KNO_3 crystals within the same crystal phase.³⁶ This occurrence was explained on the basis of the blueshift of the one-phonon DOS with increasing pressure which modulates the efficiency of the main relaxation channel: the down-conversion processes to the ν_2 state.

In benzene the relaxation dynamics of the ν_1 vibrational mode is dominated at low temperature and room pressure by down-conversion processes to the ν_{10} mode at $\sim 860 \text{ cm}^{-1}$.^{37,38} As the temperature increases up-conversion processes become more important and the coupling to the ν_{18} mode (1037 cm^{-1}), driven by lattice phonons of suitable energy ($\sim 40 \text{ cm}^{-1}$), is identified as one of the main relaxation channels. The pressure increase induces a blueshift of the phonon DOS, and the temperature increase determines an

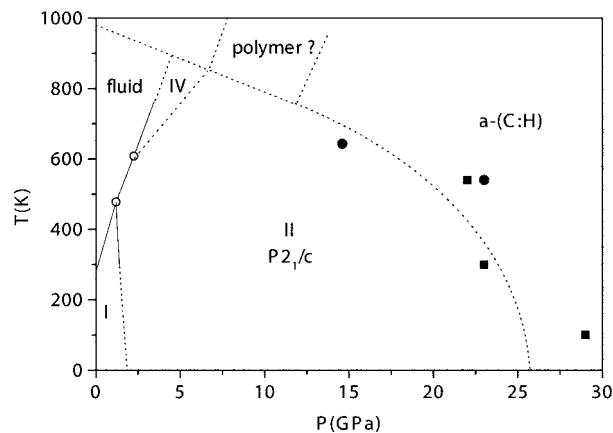


FIG. 8. The phase diagram of benzene as it results from the present work. The full lines, identifying the melting line and the I-II phase boundary, and the two triple points (empty circles) are from Ref. 22. Dashed lines delimit the hypothesized phase IV, the low-temperature region of phase I, and the stability range of benzene (Ref. 15). Full squares indicate the reaction threshold pressure we have observed in the present (540 K) and previous works (Ref. 16). It should be remarked that while the reaction at 540 K occurs from annealed phase II samples, the data from Ref. 16 refer to not-annealed samples.

analogous shift of the population distribution. The net result is that, due to the low energy of the phonon assisting the up-conversion process to the ν_{18} mode, this contribution to the line broadening could decrease with increasing pressure thus explaining the line narrowing during the compression. Following this pressure tuning of the one-phonon DOS new relaxation channels can be opened determining a line broadening at higher pressures. Even less reliable is the identification of the III-III' phase transition where only a slight slope change is observed,¹⁵ since the assumption of a linear evolution of the full width at half maximum with pressure is not justified.

Following this discussion, and on the basis of our x-ray results, the phase diagram of benzene appears greatly simplified (Fig. 8). High-temperature studies should be performed to test the existence of phase IV, which was only presumed,¹⁵ and to study the products of the high-temperature reactions, since the formation of other polymeric networks different from the amorphous hydrogenated carbons obtained below 600 K was claimed and related to the different crystal structures from which the reaction was induced.

VI. CONCLUSIONS

The study of crystalline benzene at high temperature and pressure by ir and x-ray diffraction allowed us to gain information on the crystal structure and on the phase diagram. The ir measurements are a powerful probe for monitoring the annealing procedure to remove metastable crystalline domains of phase I in the high-pressure phase II. The

diffraction data collected on high-quality powdered samples allowed the structure of phase II to be identified as $P2_1/c$. This phase is stable up to the occurrence of the chemical reaction thus simplifying the existing phase diagram. Different annealed samples present small differences of the crystal parameters, reflecting the nonhydrostatic compression conditions and possible different preferential orientations, that do not affect the main structural information.

ACKNOWLEDGMENTS

The authors gratefully acknowledge the staff of ID30 at ESRF for the assistance in the measurements. We also thank J. Haines for useful discussions on the x-ray data analysis. This work has been supported by the European Union under Contract No. HPRI-CT1999-00111 and by the Italian Ministero dell'Università e della Ricerca Scientifica e Tecnologica (MURST).

*Electronic address: gorelli@lens.unifi.it

†Electronic address: santoro@lens.unifi.it

‡Electronic address: bini@chim.unifi.it

¹P. F. McMillan, *Nat. Mater.* **1**, 19 (2002).

²V. Schettino, R. Bini, *Phys. Chem. Chem. Phys.* **5**, 1951 (2003).

³R. Bini, *Acc. Chem. Res.* **37**, 95 (2004).

⁴M. Citroni, M. Ceppatelli, R. Bini, and V. Schettino, *Science* **295**, 2058 (2002).

⁵D. Chelazzi, M. Ceppatelli, M. Santoro, R. Bini, and V. Schettino, *Nat. Mater.* **3**, 470 (2004).

⁶M. Sakashita, H. Yamawaki, and K. Aoki, *J. Phys. Chem.* **100**, 9943 (1996).

⁷M. Ceppatelli, M. Santoro, R. Bini, and V. Schettino, *J. Chem. Phys.* **113**, 5991 (2000).

⁸Ph. Pruzan, J. C. Chervin, M. M. Thiéry, J. P. Itié, and J. M. Besson, *J. Chem. Phys.* **92**, 6910 (1990).

⁹S. Block, C. E. Weir, and G. J. Piermarini, *Science* **169**, 586 (1970).

¹⁰M. Nicol, M. L. Johnson, and N. C. Holmes, *Physica B & C* **139-140**, 582 (1986).

¹¹M. M. Thiéry and J. M. Legér, *J. Chem. Phys.* **89**, 4255 (1988).

¹²M. M. Thiéry, J. M. Besson, and J. L. Bribes, *J. Chem. Phys.* **96**, 2633 (1992).

¹³J. M. Besson, M. M. Thiéry, and P. Pruzan, in *Molecular Systems Under High Pressure*, edited by R. Pucci and G. Piccitto (Elsevier, Amsterdam, 1991), p. 341.

¹⁴M. Gauthier, J. C. Chervin, and P. Pruzan, in *Frontiers of High Pressure Research*, edited by H. D. Hochheimer and R. D. Etters (Plenum Press, New York, 1991), p.87.

¹⁵F. Cansell, D. Fabre, and J. P. Petit, *J. Chem. Phys.* **99**, 7300 (1993).

¹⁶L. Ciabini, M. Santoro, R. Bini, and V. Schettino, *J. Chem. Phys.* **116**, 2928 (2002).

¹⁷L. Ciabini, M. Santoro, R. Bini, and V. Schettino, *Phys. Rev. Lett.* **88**, 085505 (2002).

¹⁸B. R. Jackson, C. C. Trout, and J. V. Badding, *Chem. Mater.* **15**,

1820 (2003).

¹⁹E. G. Cox, D. W. J. Cruickshank, and J. A. S. Smith, *Proc. R. Soc. London, Ser. A* **247**, 1 (1958).

²⁰G. E. Bacon, N. A. Curry, and S. A. Wilson, *Proc. R. Soc. London, Ser. A* **279**, 98 (1964).

²¹G. J. Piermarini, A. D. Mighell, C. E. Weir, and S. Block, *Science* **165**, 1250 (1969).

²²J. Akella and G. C. Kennedy, *J. Chem. Phys.* **55**, 793 (1971).

²³W. D. Ellenson and M. Nicol, *J. Chem. Phys.* **61**, 1380 (1974).

²⁴D. M. Adams and R. Appleby, *J. Chem. Soc., Faraday Trans. 2* **73**, 1896 (1977).

²⁵M. M. Thiéry, D. Fabre, I. L. Spain, and K. Kobashi, *Physica B & C* **139-140**, 520 (1986).

²⁶A. Anderson, B. Piwowar, and W. Smith, *Spectrosc. Lett.* **31**, 1811 (1999).

²⁷L. Ciabini, M. Santoro, R. Bini, and V. Schettino, *J. Chem. Phys.* **115**, 3742 (2001).

²⁸H. K. Mao, P. M. Bell, J. V. Shaner, and D. J. Steinberg, *J. Appl. Phys.* **49**, 3276 (1978).

²⁹R. Bini, R. Ballerini, G. Pratesi, and H. J. Jodl, *Rev. Sci. Instrum.* **68**, 3154 (1997).

³⁰F. A. Gorelli, L. Ulivi, M. Santoro, and R. Bini, *Phys. Rev. Lett.* **83**, 4093 (1999).

³¹A. P. Hammersley, computer code FIT2D (ESRF, 1998).

³²M. M. Thiéry, and C. Rérat, *J. Chem. Phys.* **104**, 9079 (1996).

³³P. Vinet, J. Ferrante, J. R. Smith, and J. H. Ross, *J. Phys. C* **19**, 467 (1986).

³⁴M. Baggen, M. van Exter, and A. Lagendijk, *J. Chem. Phys.* **86**, 2423 (1986).

³⁵S. Califano and V. Schettino, *Int. Rev. Phys. Chem.* **7**, 19 (1988).

³⁶M. Jordan, A. Schuch, R. Righini, G. F. Signorini, and H. J. Jodl, *J. Chem. Phys.* **101**, 3436 (1994).

³⁷R. G. Della Valle and R. Righini, *Chem. Phys. Lett.* **148**, 45 (1988).

³⁸R. Torre, R. Righini, L. Angeloni, and S. Califano, *J. Chem. Phys.* **93**, 2967 (1990).